# Assimilation of radiance data at JMA: recent developments and prospective plans

***Kozo Okamoto, Hiromi Owada, Takumu Egawa and Toshiyuki Ishibashi***

*Japan Meteorological Agency (JMA), Tokyo, Japan*

## Abstract

Recent developments on the satellite data assimilation at JMA, especially regarding radiance data, are presented. After the last conference in October 2006, JMA introduced various data into its operational global 4D-Var data assimilation system. The data include: AP-RARS/EARS ATOVS radiances, ATOVS radiances onboard NOAA18 and Metop, MTSAT-1R water vapor clear sky radiances (WV-CSRs), and refractivities of CHAMP GPS radio occultation. Above all, Metop ATOVS (AMSU-A and MHS) gave the greatest positive impact on forecasts, especially of geopotential height, in our data assimilation experiments. AIRS radiance assimilation is under development: The evaluation of cloud detection scheme against CloudSat and that of analysis against radiosondes was encouraging but, at the time of writing, the forecast skill was degraded due to the discrepancy between the model trend and AIRS impact. The improvement of a cloud screening and bias correction for SSMI, TMI and AMSR-E and the inclusion of SSMIS radiances at window channels were evaluated. Appropriate usage of frequent measurements of WV-CSRs from five geostationary satellites generated greater positive impact on forecast than from MTSAT-1R only.

## Outline of JMA NWP system

JMA operates two deterministic forecast models: the global spectral model (GSM) and mesoscale model (MSM, Japan Meteorological Agency 2007). GSM was significantly upgraded in November 2007. The resolution was upgraded from TL319L40 to TL959L60 (roughly 20 km in horizontal resolution) and model top height was raised from 0.4 hPa to 0.1 hPa. This upgrade improved forecast of severe precipitation and various synoptic fields including 500 hPa geopotential height (Z500) and wind speed at 250 and 850 hPa in the extra-tropics and tropics.

The global data assimilation system is based on incremental 4D-Var with the resolution of TL319L40/T106L40 to TL959L60/T159L60 in the outer/inner loop. 6-hour assimilation window is divided into six time slots of about 1-hour. The early and delayed (cycle) global analysis are operated in JMA. Data cut-off time is set to 2h25m for the early analysis, and 5h35m and 11h35m for the cycle analysis at 00/12 UTC and 06/18 UTC, respectively. The early analysis is followed by 84-h forecast at 00, 06 and 18 UTC and 192-h forecast at 12 UTC. Variational Bias Correction (VarBC, Derber and Wu 1998; Dee 2004) is applied for all radiance data assimilated in the global 4D-Var.

MSM aims at providing the disaster prevention information such as heavy rain prediction around Japan. It is a non-hydrostatic grid model with a horizontal resolution of 5 km and 50 vertical layers up to about 22 km (Saito et al. 2006). MSM operates every three hours and performs 15-h forecast at 00/06/12/18 UTC and 33-h forecast at 03/09/15/21 UTC. The assimilation system of MSM is an incremental 4D-Var method with the resolution of 10/20 km in the outer/inner loop. Assimilation window is six hours with six 1-hour time slots and data cut-off time is 50 minutes. While the global 4D-Var system assimilates radiances from various satellites, the meso 4D-Var system assimilates retrievals due to the smaller computational burden required for the strict operational time schedule. The radiance assimilation in the meso 4D-Var system is under development considering the availability of VarBC.

The satellite data operationally assimilated in the global (G) or meso (M) analysis systems are as follows (as of May 2008):

- NOAA15-18/AMSU-A, AMSU-B and MHS radiances (G)
- Metop/AMSU-A and MHS radiances (G)
- Aqua/AMSU-A radiances (G)
- NOAA15-18/ATOVS temperature retrievals, processed by NESDIS and Meteorological Satellite Center (MSC) of JMA (M)
- Metop/ATOVS temperature retrievals (M)
- DMSP-13,-14/SSMI radiances (G), and total column water vapor (TCWV) and rain rate (M)
- TRMM/TMI radiances (G), and TCWV and rain rate (M)
- Aqua/AMSR-E radiances (G), and TCWV and rain rate (M)
- MTSAT-1R, GOES-11,-12, and Meteosat-7,-9 AMV (G and M)
- Aqua/MODIS and Terra/MODIS AMV (G)
- QuikSCAT Sea surface winds (G and M)

The following sections are confined to the radiance assimilation in the global analysis.

## ATOVS radiance assimilation

Changes in ATOVS radiance assimilation in the global analysis since the last TOVS conference in October 2006 are the addition of the Asia-Pacific Regional ATOVS Re-transmission System (AP-RARS) in February 2007, NOAA18 in April 2007, EUMETSAT Advanced Retransmission Service (EARS) in August 2007 and Metop in November 2007. We assimilate AP-RARS from 12 stations in Australia (5), China (4), Korea (1) and Japan (2), including Japan's Syowa Station on the Antarctica, as of May 2008. The assimilations of Metop and RARS are shown in this section.

The level-1C data of AMSU-A and MHS on Metop from EUMETSAT via GTS became available at JMA on 7 February 2007. The stability and timeliness of the data dissemination, which are essential for an operational NWP system, have been entirely satisfactory. They are pre-processed and

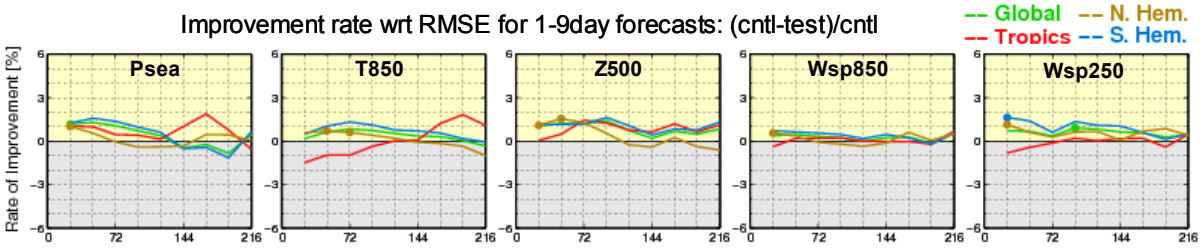


Fig. 1: Forecast improvement rate (error reduction rate) with respect to the root mean square forecast error (RMSFE) when adding AMSU-A and MHS on Metop for sea surface pressure (Psea), temperature at 850 hPa (T850), geopotential height at 500 hPa (Z500), wind speed at 850 hPa (Wsp850) and 250 hPa (Wsp250). The improvement rate is RMSFE difference of the run with Metop (test) from the run without Metop (cntl) normalized by cntl RMSFE, being positive for smaller RMSFE in test. It is calculated over a month in June 2007 for the Northern Hemisphere (brown lines), Tropics (red), Southern Hemisphere (blue) and the globe (green), and dots on lines represent the statistical significance.

assimilated as ATOVS radiances on NOAA satellites are done (Okamoto et al. 2006). The cycle experiments with Metop/ATOVS radiances showed substantial positive impacts on forecast at day 1 to day 3, especially for the geopotential height even in the presence of four NOAA satellites (NOAA15-18) and Aqua satellites (Fig.1).

The use of the early delivery ATOVS data from AP-RARS and EARS in the early global analysis makes the analysis closer to the cycle global analysis. The early analysis generating forecast products are not allowed to wait for sufficient satellite data coming in. In contrast, because the cycle analysis assimilates more satellite data due to longer data cut-off time length, it is generally more accurate than the early analysis. In order to assess impacts of AP-RARS and EARS individually, three one-month early analysis experiments were carried out: "EXP-NORARS" run where operational data configuration was used, "EXP-APRARS" run where AP-RARS ATOVS data were added to EXP-NORARS, and "EXP-EARS" run where EARS ATOVS data were added to EXP-NORARS.

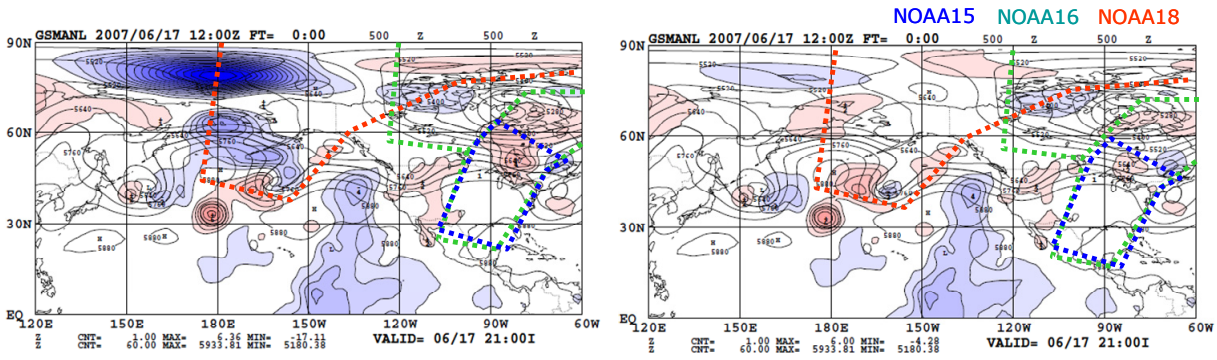


Fig. 2: Difference between early analysis and cycle analysis for Z500 (left) without EARS ATOVS and (right) with EARS ATOVS at 12 UTC on 17 June 2007. Blue (red) shades depict positive (negative) value of the difference and contours indicate Z500. Outlines of ATOVS data coverage are plotted with dashed lines.

EXP-APRARS showed a better fit to cycle analysis with respect to the geopotential height mostly in the stratosphere around AP-RARS stations than in EXP-NORARS. Meanwhile, EXP-EARS showed much better agreement with the cycle analysis for Z500 in the mid- and high-latitudes of the Northern Hemisphere (Fig.2) and better forecasts in the Northern Hemisphere and Tropics than EXP-NORARS (not shown). The greater impact of EARS on forecast were due to the number of EARS ATOVS data available, which was generally three times more than that of AP-RARS ATOVS data.

## AIRS radiance assimilation

The assimilation of the hyperspectral infrared sounder AIRS onboard Aqua is being developed. We are receiving AIRS warmest field of view (FOV) dataset with 324 channels from NESDIS. Clear radiances of 54 temperature sounding channels, which are chosen based on an entropy reduction method (Rodgers 2000), have been tested over the ocean. The data are thinned to one per a 180 x 180 km box by giving the priority to pixels closer to the center of the box and analysis time, and go to subsequent quality control (QC) and bias correction (BC) procedures. The primary QC procedure is the rejection of cloud-contaminated channels. The cloudy channel identification consists of two steps. First, completely clear pixels, of which no channels are contaminated by clouds, are identified with different approaches at daytime and nighttime. At daytime, pixels with cloud fraction less than 10 % are determined to be completely clear. The cloud fraction is derived from the visible and near infrared channels and is included in the data. At nighttime pixels are flagged as completely clear on condition that 1) their brightness temperature (TB) differences between short wavelength channel and long wavelength channel are small (i.e. neither low clouds nor thin cirrus are present) and 2) sea surface temperature (SST) simulated from window channels is close to SST given by independent SST analysis (i.e. no thick clouds are present, Le Marshall et al 2006). Second, if the pixels are not completely clear, clear channels are determined using McNally and Watts (2003). Even clear pixels are removed when observation-minus-background (O-B) exceeds three times the observation errors predefined or any instrumental quality error flags included in the data are on. The BC scheme adopts the same method as ATOVS except VarBC predictors.

A cloud top height (CTH) can be estimated from cloudy channels identified with the altitude of their weighting functions. We verified the AIRS CTH with the Cloud Profiling Radar (CPR) on CloudSat satellite (Stephens et al. 2002). Figure 3 (a) shows frequency of CTH from CRR in 2B-GEOPROF dataset with cloud mask over 30 at every two pixels and that from QC-passed AIRS over the ocean. A population at 0.5 km height indicates clear pixels. The lower rate of low clouds at 1-2 km altitude in AIRS suggests that AIRS may miss those clouds because passive infrared instruments have difficulty distinguishing radiations from the ground and low clouds. In contrast, higher rate of mid-level clouds at 3-5 km from AIRS is evident. The reason is not clear but it may be associated with dry biases of the model because the current cloud detection algorithm is based on O-B variation with height.

Figure 3 (b) is a scatter plot of CTH from QC-passed AIRS and that from CPR closest to the center of

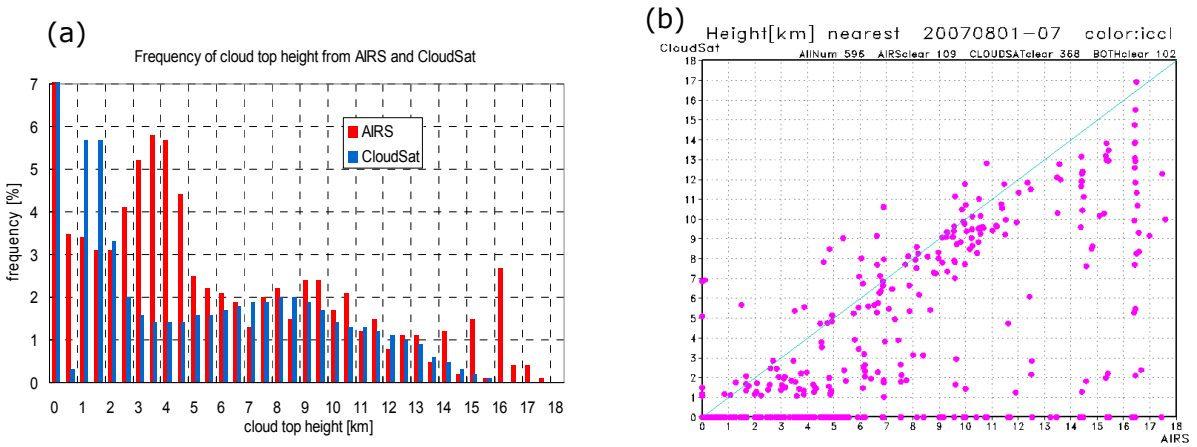


Fig. 3: (Left) Frequency of cloud top height from AIRS and CloudSat/CPR (2B-GEOPROF) from 1 to 7 2007. The frequency is normalized by their total number. (Right) Comparison of cloud top height from AIRS and that from CloudSat/CPR closest to the center of AIRS FOV from 1 to 7 2007.

the AIRS FOV. While some AIRS CTHs well agree with CPR CTHs, not a few AIRS CTHs are higher than CPR CTHs. This can be explained by the fact that AIRS is more sensitive to small cloud particles. Moreover, the figure shows that there are many pixels flagged as cloud for AIRS but as clear for CPR. This is probably because, in addition to the sensitivity difference, much smaller CPR FOV can spot a clear portion in a broken cloud area while AIRS radiance can be affected by partial clouds. From these comparisons, it is hard to conclude that AIRS CTH is accurate enough for a pure CTH retrieval purpose but the algorithm to identify cloudy channels is safer for removing cloud-affected channels in the data assimilation context of our target.

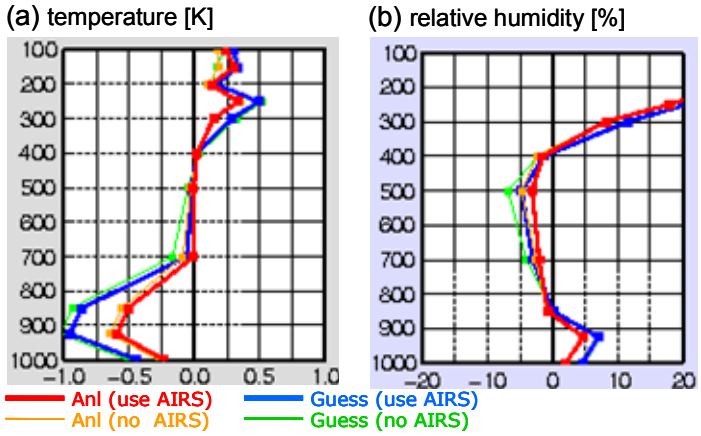


Fig. 4: Fit of analysis/first-guess to RAOBs with and without AIRS radiance assimilation for (a) the temperature in the Southern Hemisphere and (b) the relative humidity in the tropics over a month in August 2007.

AIRS radiances that underwent the QC and BC procedures were assimilated in the experimental global analysis system for 50 days from 20 July to 9 August in 2007 to evaluate their impacts on analysis and forecast. Because number of total channels of AIRS assimilated in each analysis is roughly three times more than that of AMSU-A on a single satellite, the assimilation made large changes to analyses. The large changes are found in the latitudes of 10S to 30N in the mid-troposphere and tropospheric temperature in the southern hemisphere and stratospheric temperature (not shown). Reflecting these changes, biases in the lower tropospheric temperature in the southern hemisphere and

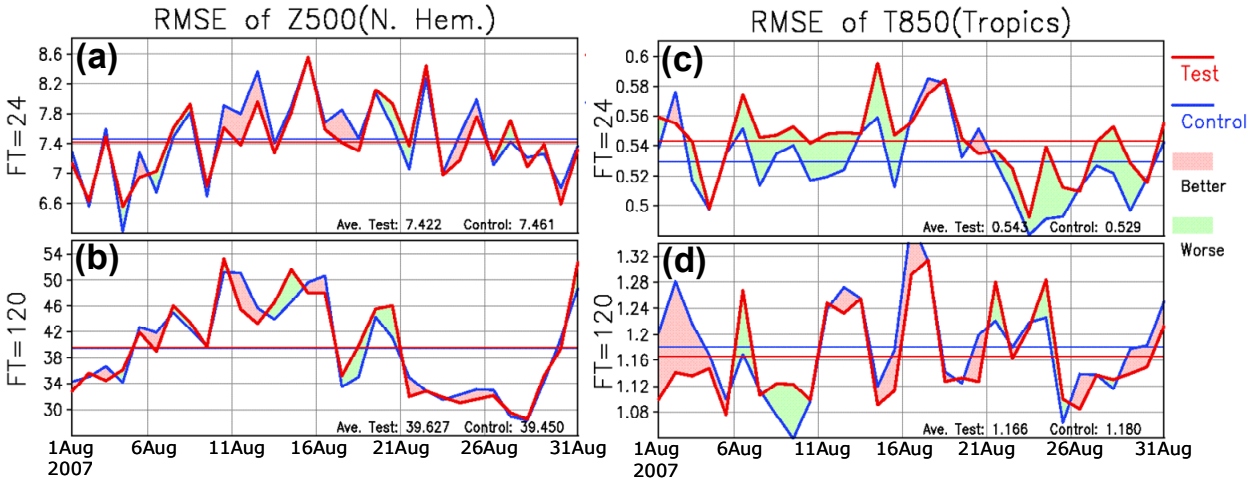


Fig. 5: Time sequence of RMSFE at day-1and -5 initialized on 1-31 Aug, 2007for Z500 (a, b) and T850 (c, d). Test run assimilates AIRS radiances and Control run does not.

mid-tropospheric humidity in the tropics verified against radiosonde observation (RAOB) are significantly reduced (Fig.4). However impacts on the day-1 forecast verified against their own initials are neutral for Z500 and negative for temperature at 850hPa (T850) (Fig. 5). Moreover, moistening the mid troposphere caused excessive precipitation in the tropics (not shown). These detrimental effects might be due to the conflict between model biases and analysis increment by AIRS. We are tackling this conflict by reviewing the bias correction procedure, re-estimation of observation errors as well as model physical process in the GSM.

## MicroWave Imager (MWI) radiance assimilation

Less-cloud affected radiances from microwave imagers such as SSMI, TMI and AMSR-E have been assimilated over the ocean operationally since May 2005. Only vertical polarized channels are assimilated because we believe that there is little independent information in horizontal polarized channels in our system where no Jacobian with respect to the surface parameters, such as temperature or wind speed, is included. The removal of cloud affected radiances is implemented using three cloud-related indices of CWI, $S_{IDX}$ and $P_{IDX}$. CWI is calculated from TB at 19 and 37 GHz channels, SST and ocean surface emissivity (Takeuchi 2002). $S_{IDX}$ and $P_{IDX}$ are

$$S_{IDX}=(T22V\text{-}T37V) - C_S(T22V\text{-}T19V)$$

$$P_{IDX}=(T85H/T85V) - C_P(T22V\text{-}T19V),$$

where $TxV$ ($TxH$) is TB observed at vertically (horizontally) polarized channel at frequency $x$, and the coefficients $C_S$ and $C_P$ are estimated for each instrument. These indices go beyond certain ranges when rain or clouds are present. In addition to excluding cloudy radiances, data are screened out when O-B in TB is over three times the predefined observation error or O-B in TCWV is over 10 mm. Biases are corrected by VarBC with predictors of TCWV, sea surface temperature (SST), square of SST, ocean surface wind speed, $1/\cos\theta$ ($\theta$ is a satellite zenith angle) and constant parameter.

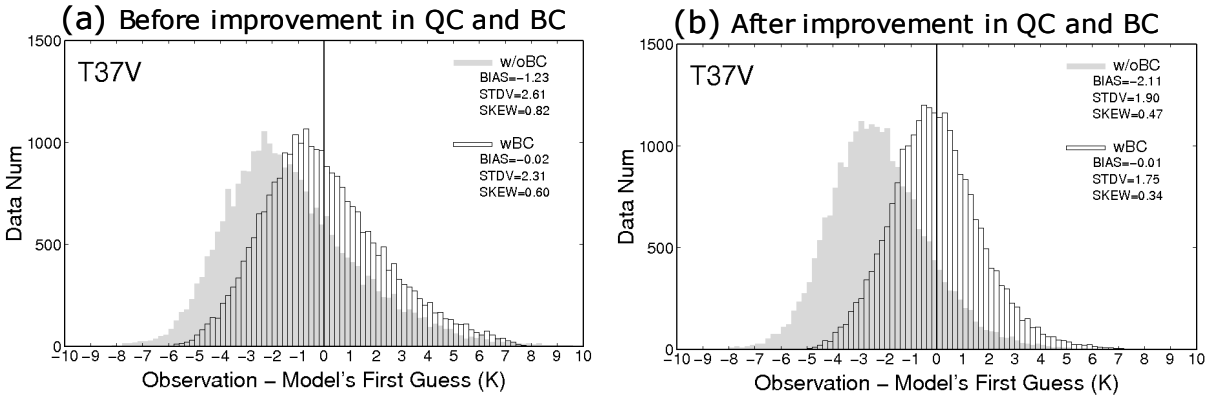


Fig. 6: O-B frequency of AMSR-E 37V in the clear condition over the ocean on 1st August 2007 (a) before and (b) after improved QC and BC.

It was found that cloudy radiances still remained and biases were not sufficiently removed at 37 GHz channel even after these QC and BC procedures were applied. Figure 6 (a) shows that O-B in TB after the cloud screening over the ocean has larger populations in a positive tail, indicating observed TB is higher than background calculated in clear conditions due to the additive radiation from clouds. The figure also shows that bias corrected O-B is not centered around zero. With a view of making the cloud screening stricter, a cloud test was added which identifies cloudy radiances when total column cloud liquid water (TCCLW) retrieved from Takeuchi (2002) was beyond 0.18 kg/m$^2$. To improve the bias correction, furthermore, TCCLW retrieved was included in VarBC predictors instead of $1/\cos\theta$. These revisions made O-B distribution more symmetric and the bias correction better (Fig. 6 (b)). With two month assimilation experiments in summer and winter times, they slightly but consistently improved the forecast of the lower tropospheric temperature (not shown). Because the criteria of 0.18 kg/m$^2$ might allow cloud contaminated data in the 85 GHz bands to survive, we are testing frequency dependent criteria (Okamoto and Derber 2006). They are planned to be introduced in the operational global analysis in 2008 or early 2009.

SSMIS window channels (19V, 22V, 37V and 92V) on DMSP-16 were experimentally assimilated together with the new cloud screening and VarBC predictors above. Quality controlled O-B mean and standard deviation (STD) from SSMIS were nearly equal to those from other MWIs already assimilated. Impact of the addition of SSMIS window channel radiances on the analysis and forecast were small and neutral. Assimilating radiances from sounding channels of SSMIS in the global analysis system and TCWV and rain rate retrievals in the meso analysis system are under development.

## Clear sky radiances of water vapor channels of geostationary satellite imagers

Clear sky radiances of the water vapor channel (WV-CSRs) of MTSAT-1R imager has been

operationally assimilated since June 2007. They are thinned to one in 200 km box and every other time slot so that horizontal and temporal error correlation could be neglected in 4D-Var. The QC procedure removes WV-CSR data with clear portion less than 35 % or TB STD over 1K, which are generated from 16x16 original pixels by MSC of JMA. The data with O-B in excess of 3K are screened out. Biases are removed with VarBC with predictors of background TB, jet level wind speed, $1/\cos\theta$ and constant parameter.

To evaluate impact of WV-CSR assimilation, three cycle experiments were carried out with the low resolution (TL319L60) global analysis system over 50 days in summer and winter seasons: 1) "EXP-NOCSR" run using no WV-CSRs, 2) "EXP-MTSAT" run using MTSAT-1R WV-CSRs in addition to EXP-NOCSR and 3) "EXP-5GEO" run using WV-CSRs of five geostationary satellites of MTSAT-1R, GOES-11, -12 and METEOSAT-7, -9 in addition to EXP-NOCSR. EXP-MTSAT showed small but positive impact on analysis (e.g. smaller O-B STD of NOAA18/MHS channel 3) and neutral to small positive impact on forecast (Fig. 7 (a)). EXP-5GEO yielded more positive impact: TCWV was increased in the mid- to upper-troposphere in wet areas and even in the lower-tropospheric in dry areas such as Sahara. This was likely caused by frequent measurements even over the land, which compensated microwave imagers. The humidity increase reduced the dry biases of the model: Analysis/guess humidity was closer to RAOB at 500 to 250 hPa and O-B STD of MHS and AMSU-B channel 3 was down. Improvement was obvious for T850, Z500 and wind speed at 850 and 250 especially at day 1 to 3 forecast (Fig. 7 (b)).

However, the use of WV-CSRs from MTSAT-1R has been suspended due to technical reasons since November 2007 when GSM was upgraded. It is planned that WV-CSRs from five geostationary satellites are introduced in the operational global analysis in mid 2008.

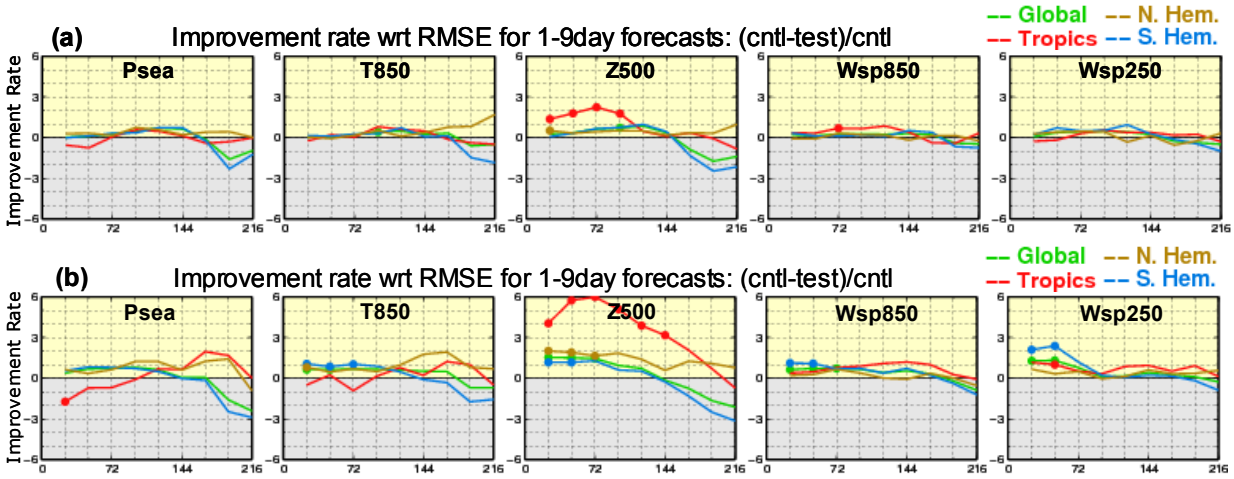


Fig. 7: Improvement rate in (a) EXP-MTSAT run and (b) EXP-5GEO.

## Summary and Plan

JMA introduced in the global analysis AMSU-A and MHS radiances on NOAA18 and Metop, AMSU-A and MHS radiances from AP-RARS and EARS, refractivity from CHAMP and WV-CSR from MTSAT-1R since the last TOVS conference in October 2006. AMSU-A and MHS radiances from Metop yielded the greatest positive impact of these data probably due to the complementary orbital coverage to fill the gaps of NOAA and Aqua satellites, good stability and timeliness as well as the accuracy.

Ongoing developments with radiance assimilation in the global analysis are assimilating cloudy/rainy radiances, utilizing more data over land by introducing more accurate estimate of the land emissivity, optimizing observation errors in the variational scheme, reevaluating a thinning distance and improving a vertical interpolation method. In the meso analysis, radiance assimilation is planned to be implemented together with VarBC instead of the retrieval assimilation.

## References


Dee, D. P., 2004: Variational bias correction of radiance data in the ECMWF system. *Proceedings of the ECMWF workshop on assimilation of high spectral resolution sounders in NWP. Reading, UK. 28 June - 1 July 2004.*

Derber, J.C., and W.-S Wu, 1998: The use of TOVS cloud-cleared radiances in the NCEP SSI analysis system. *Mon. Wea. Rev.*, **126**, 2287-2299.

Japan Meteorological Agency, 2007: Outline of the operational numerical weather prediction at the Japan Meteorological Agency. Appendix to WMO numerical weather prediction progress report, available on http://www.jma.go.jp/jma/jma-eng/jma-center/nwp/outline-nwp/index.htm

Le Marshall, J., J. Jung, J. Derber, M. Chahine, R. Treadon, S. Lord, M. Goldberg, W. Wolf, H.C. Liu, J. Joiner, J. Woollen, R. Todling, P. van Delst, and Y. Tahara, 2006. Improving Global Analysis and Forecasting with AIRS. *Bull. Amer. Meteor. Soc.*, **87**, 891-894.

Okamoto, K., H. Owada, Y. Sato, and T. Ishibashi, 2006: Use of satellite radiances in the global assimilation system at JMA. *Proceedings of the 15th International TOVS Study Conference, Maratea, Italy, 4-10 October 2006.*

Okamoto, K. and J. C. Derber, 2006: Assimilation of SSM/I radiances in the NCEP global data assimilation system. *Mon. Wea. Rev.*, **134**, 2612-2631.

Rodgers, C. D., 2000: Inverse methods for atmospheric sounding: Theory and Practice, World Scientific, 238pp.

Saito, K., J. Ishida, K. Aranami, T. Hara, T. Segawa, M. Narita, and Y. Honda, 2007: Nonhydrostatic atmospheric models and operational development at JMA. *J. Meteor. Soc. Japan*, **85B**, 271-304.

Saunders, R., P. Brunel, F. Chevallier, G. Deblonde, S. English, M. Matricardi, and P. Rayer, 2002: RTTOV-7 science and validation report. available on http://www.metoffice.com/research/interproj/nwpsaf/rtm/rttov7_svr.pdf

Stephens, G. L., D. G. Vane, J. B. Ronald, Gerald G. Mace, Kenneth Sassen, Zhien Wang, Anthony J.

Illingworth, E. J. O'Connor, W. B. Rossow, S. L. Durden, S. D. Miller, R. T. Austin, A. Benedetti, C. Mitrescu, and the CloudSat Science Team, 2002: The CLOUDSAT mission and the A-TRAIN. a new dimension of space-based observations of clouds and precipitation. *Bull. Amer. Meteor. Soc.*, **83**, 1771-1790.

Takeuchi, Y., 2002: Algorithm theoretical basis document (ATBD) of the algorithm to derive total water vapor content from ADEOS-II/AMSR, available on http://sharaku.eorc.jaxa.jp/AMSR/doc/alg/4_alg.pdf